

The emerging digital radiology

J. J. Pedroso de Lima

IBILI - Biofísica/Biomatemática - Fac. Med. Univ. Coimbra

Resumo - É analisada a evolução das técnicas digitais da radiologia nas últimas décadas, considerando-se as diferentes aproximações desde a utilização do tubo intensificador de imagem até aos modernos detectores de selénio amorfo. Consideram-se as propriedades mais importantes dos detectores na perspectiva de satisfazer as exigências das imagens radiológicas (campo, características geométricas, eficiência quântica, espessura do detector, gama de resposta, ruído, eficiência extrínseca, eficiência total e eficiência quântica de detecção). Aspectos relevantes associados com a transferência de informação são analisados com algum detalhe. Consideram-se as respostas dos sistemas presentemente disponíveis em termos de eficiência quântica de detecção (DQE), demonstrando-se que os detectores de estado sólido (silício amorfo) são, no presente, os mais favoráveis.

Abstract - The evolution of radiological digital techniques in the last decades is analysed taking into account the different approaches from the image intensifier tube to the modern amorphous-selenium area detectors. The important properties of image detectors in the perspective of fulfilling the needs of images in radiology (field coverage, geometrical characteristics, quantum efficiency, detector thickness, dynamic range, noise, detector extrinsic efficiency, detector total efficiency and detective quantum efficiency) are considered. Some relevant points associated with information transfer are referred with some detail. The response characteristics of the presently available systems in terms of detective quantum efficiency are analysed and it is showed that amorphous silicon solid-state detectors are the most appropriate.

I INTRODUCTION

Digital images are not man's invention. The patterns in butterfly wings are digital images stored in the genetic information, kept in the base-pair sequences of DNA molecules. Fig. 1 is just an example in thousands.

Besides, digital radiology is not new. CT scanning proposed by Hounsfield in 1973 and topogram, its



Fig. 1 - The patterns in butterfly wings are digital images stored in DNA molecules

complementary technique, are true digital methodologies in use since the seventies. Also techniques that digitise the output from image intensifier tubes such as CR (Computerised radiology - fluorography and fluoroscopy) and DSA (digital subtraction angiography), after an initial stage, are digital techniques.

Recent developments in filmless diagnostic radiology led to devices that deal digitally with the information right from the acquisition. These new X-ray images are based upon properties of solid state and luminescent materials.

As shown in Fig.2 a unique characteristic of conventional film-screen X-ray systems is that they combine detector and display functions in the film.

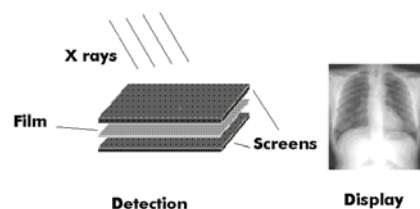


Fig. 2 - Detection and display functions in the X-ray film.

In modern digital radiography the computer separates the two functions, detection and display. The most interesting consequence of this is the inherent capacity

of digital systems to manipulate data for image optimisation.

II. DIGITAL TECHNIQUES CHARACTERISTICS

A number of characteristics can be associated to digital techniques as advantages with respect to screen/film conventional mode. In fact these techniques allow:

- Data and image processing: contrast enhancement, parameter evaluation (distances, angles, areas), etc.
- Revaluation with reprocessing
- Elimination of film and chemistry, i.e., electronic images without film development delays
- Information transmission for direct utilisation in other areas (radiotherapy, surgery,).
- Decrease in patient absorbed dose
- Electronic storage and retrieval of image (space saving and fast consultation)
- Telediagnosis through digital communication
- Utilisation of artificial intelligence (expert systems for supported functions)
- Simultaneous visualisation, comparison and coregistration of multimodal images.

Other limitations of film recording comparing to modern digital techniques are:

- Small dynamic range
- Poor contrast - ~5% differences visible (this represents our contrast sensitivity $\Delta B/B$; B - luminance)
- Small quantum efficiency - film/screen absorbs only 20-40 % of available X-ray photons
- Not easily transferable to digital storage
- Expensive at long term although smaller initial investment.

III. DIGITAL RADIOLOGY SOURCES

The sources of digital radiology images are:

- Film digitalisation - not interesting
- Image intensifier - Computerised Radiology (Digital fluoroscopy, digital fluorography and digital subtraction); TV camera (CCD, vidicon or saticon)
- Digital acquisition with semiconductor, phosphors and gas detectors - CT and new digital systems.

IV. IMPORTANT DETECTOR PROPERTIES

In order to fully analyse the qualities of the different detection systems available it is important to take into account several related properties: field coverage, geometrical characteristics, quantum efficiency, sensitivity, spatial resolution, noise characteristics,

dynamic range, uniformity, acquisition speed, frame rate and cost.

A. Field coverage

The detector of the imaging system must be able to record the X-ray transmitted over the projected anatomic area under investigation. Chest radiography requires an imaging field 35x43 cm while mammography needs a receptor of dimensions 18x24 cm or 24x30 cm. Image intensifiers provide circular fields with diameters from 15 to 40 cm.

B. Geometrical characteristics

Dead regions exist in detectors:

1. Within and around the edges of detectors.
2. For routing of wire leads or placement of auxiliary units in digital radiography electronic detector components.
3. In large-area detectors by abutting smaller detector units (tiling).

Distortion occurs as a result of non-linear mapping that may become spatially or angularly dependent. An example, in Fig. 3, is 'pincushion' or 'barrel' distortion caused by image intensifier geometry.

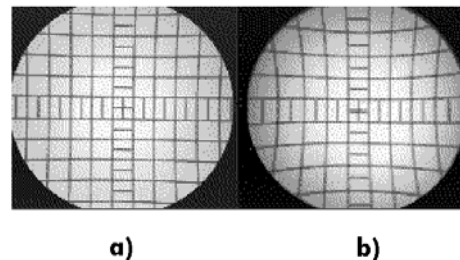


Fig. 3 - Spatial distortion in image intensifiers. a) New generation. b) Old generation.

Spatial non-uniformity is also common in most imaging devices. Due to this defect the response to uniform objects is not an uniform image (Fig. 4).

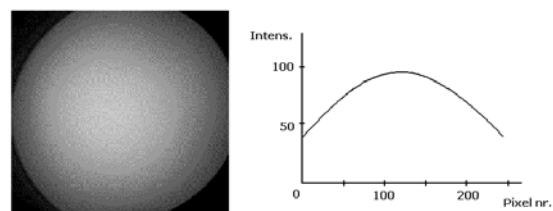


Fig. 4 - Non uniform response of a detector system to a homogeneous disc (vignetting).

C. Quantum efficiency

Quantum efficiency, η , measures the interaction probability, i.e., the fraction of incident photons that interacts with the detector, then

$$\eta = 1 - e^{-\mu x_d} \tag{1}$$

where x_d is the detector thickness and μ the linear attenuation coefficient.

Quantum efficiency depends on:

- The μ of the detector material
- The detector thickness
- The photon energy

Detector quantum efficiency is also modified by the shielding material surrounding the detector such as the input window (aluminium, glass, titanium, etc.) and any collimation or grid which absorb incident radiation, so η is modified

$$\eta = e^{-\mu_w x_w} (1 - e^{-\mu x_d}) \tag{2}$$

where x_w and μ_w are the thickness and linear attenuation coefficient of the covering thickness.

D. Detector thickness

Detector thickness is a cause of spatial resolution degradation, Fig. 5.

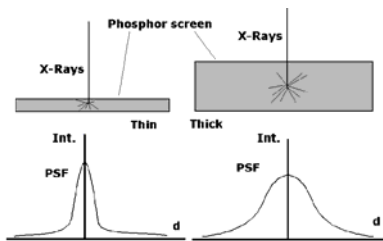


Fig. 5 - Effect of the thickness of the phosphor detector on the point spread function of a detector.

E. Dynamic range

Dynamic range (DR) is the range required to register full attenuation information,

$$DR = I_{in} / I_{out} \tag{3}$$

Since $I_{out} = I_{in} e^{-\mu x}$ and for $I_{in} = 1$

$$DR = 1 / e^{-\mu x} \tag{4}$$

The detector latitude must match the dynamic range to capture the entire contrast range. Some examples:

In mammography:

for $E_{tr} = 20 \text{ KeV}$, $\mu = 0,76 \text{ cm}^{-1}$ and $x = 6 \text{ cm}$
 $DR = 1 / e^{-4,56} = 96,33 \approx 100 : 1$

Typical film dynamic range is from 10:1 to 100:1 depending on film latitude.

Image plate displays a very wide dynamic range of about 10000:1.

F. Noise

In many situations noise is a quality-limiting factor. Fluoroscopic control in interventional radiology can take long times and then dose rate have to be small resulting in a high noise level.

The random fluctuations of X-ray intensity are Poissonian. Interaction with the detector can be considered binomial with a probability of success η .

The distribution of interacting quanta is Poisson with standard deviation

$$\sigma = (N_0 \eta)^{1/2} \tag{5}$$

N_0 is the number of events. If the detection is followed by a process with mean gain g , the signal will be

$$q = N_0 \eta g \tag{6}$$

with standard deviation

$$\sigma = [N_0 \eta (g^2 + \sigma_g^2)]^{1/2} \tag{7}$$

with σ_g the standard deviation of g .

G. Detector extrinsic efficiency

Conversion efficiency, E_c - is the fraction of absorbed photons in the detector that are converted into a measurable signal, either electrical or light. Detector extrinsic efficiency is influenced by factors such as system dead time, i.e., the time interval, after a detection, in which a detector is unable of a new detection, energy resolution and losses due to defective light coupling.

H. Detector total efficiency

Detector total efficiency is the product of quantum and extrinsic efficiency.

In intensifying screens with quantum efficiency about 0.4, conversion efficiency is about 0.5 and total efficiency is approximately 0.2.

In NaI(Tl) scintillation detectors E_Q is about 0.8 and E_C is close to 0.5. Detector total efficiency is about 0.4.

I. Detective quantum efficiency

Detective quantum efficiency (*DQE*) is defined as the square of the ratio of the output-to-input signal-to-noise ratios (*SNR*), or

$$DQE = \frac{SNR_{out}^2}{SNR_{in}^2} \quad (8)$$

SNR_{in} is obtained using the signal and noise inherent at the input X-ray distribution prior to interaction with the detector.

DQE describes the efficiency in transferring the signal to noise ratio contained in the incident X-ray pattern to the detector output, i.e., measures the combined effect of noise and contrast performance of the imaging system, as a function of spatial frequency.

DQE value especially translates one's ability to view small low contrast objects in images.

Another way, derived from its definition, to write *DQE* is

$$DQE = \frac{S_0^2 MTF(f)^2}{NPS(f)\Phi} \quad (9)$$

Where S_0 is the zero frequency signal at the detector output due to an X-ray fluency Φ at the input, $NPS(f)$ is the noise power spectrum at frequency f and $MTF(f)$ is the modulation transfer function.

This new equation indicates that *DQE* varies inversely with patient dose.

Quantum and electronic noise are unavoidable in a digital imaging chain. Noise affects drastically detectability. In many situations, to detect small objects, is more important to have high *DQE* than small resolution distance.

Compared to film/screen imaging a digital detector with high *DQE* has the potential to deliver significantly better object detectability at reduced dose.

DQE is presently the benchmark in comparing X-ray detectors. Sometimes to calculate the *DQE* of a detector it is advantageous to consider it as being composed of multiple stages, determine its value at the output of each stage and combine the results.

V. LUMINESCENCE PHENOMENA

Several types of luminescence are of major interest in imaging techniques with X and γ rays. The role of scintillators and phosphors is to emit an amount of light photons proportional to the X or γ ray energy delivered into the detector.

Three types of luminescence interest to medical imaging:

- Fluorescence
- Phosphorescence
- Thermoluminescence

Fluorescent materials have the impurity levels (traps) at the top of forbidden zone full. When X-ray interacts with the material electron generation occurs and electrons jump from valence to conduction band. Electrons from the traps at the forbidden zone fill holes in valence band emitting fluorescence characteristic light (10^{-8} - 10^{-9} s). Electrons from conduction band fall in the empty traps.

Fluorescence occurs in intensifier screens in film/screen radiography, in γ cameras and some PET and CT scanners. Also the light emission at the converter electrode in the image intensifier tube is fluorescence light.

Phosphorescent materials have empty traps at the top of forbidden zone. X-rays make electrons jump from valence to conduction band. Electrons from conduction band fall into empty traps in forbidden zone. Thermal energy can lift some of these electrons back into conduction band. Electrons from conduction band fall into holes in the valence band emitting a broad continuous light spectrum. These steps can last from 10^{-4} s to mins.

Phosphorescence phenomenon occurs in the screen of video monitors and in the output screens of image intensifier tubes.

Thermoluminescent materials have empty traps from the bottom to the top of the forbidden zone. When X-ray interacts with the material electrons jump from valence to conduction band and fall into empty traps in the forbidden zone where they stay indefinitely. Energy of excitation (heat) is necessary to eject these electrons back into the conduction band. Then they fall into the valence band emitting light photons with total energy proportional to the formerly absorbed X-ray energy.

Thermoluminescence is used in the image plates and in personal dosimeters.

VI. IMAGE INTENSIFIER

Most of digital fluoroscopy and digital fluorography systems still use an image intensifier coupled to a video camera whose output is digitised and processed. In general terms an image intensifier tube is an optoelectronic device with a photocathode that, when a light image is focused on it, is highly intensified and displayed on a second screen called visualisation screen.

The intensifier tubes used in radiology have a converter that converts the X-ray information, emerging from the patient, into a light image on the photocathode (Fig. 6).

The converter consists of an aluminium layer in contact with a fluorescent screen aimed at the production of secondary electrons by interaction with the X-rays photons emerging from the object. A fluorescent image is produced by interaction of these electrons and also by direct action of the X-rays with the fluorescent screen, (Fig. 6). The role of the Al electrode and fluorescent screen in the image intensifier is similar to the intensifier screen, in the screen-film techniques, i.e. convert

electromagnetic energy of small wavelength in light photons.

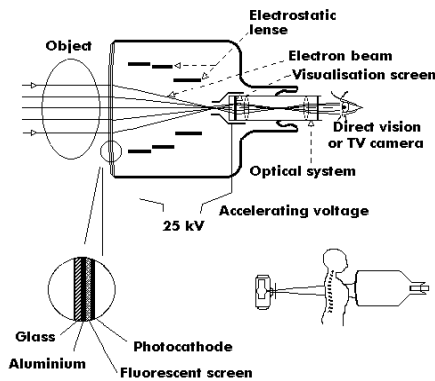


Fig. 6 - Scheme of the constitution and performance of an image intensifier tube.

The thickness of the screen is such that it represents the best compromise between X-rays absorption, with Al electrons liberation (guaranteeing an high quanta efficiency) and the dispersion of light photons (originating degradation in both contrast and spatial resolution).

The light image will induce the liberation of the photoelectrons in the photocathode that is in close contact with the fluorescent screen. Generally the photocathode surface consists of sodium antimonide, cesium iodide or zinc and cadmium sulfide.

The variations on the emerging X-rays beam intensity modulate the density of photoelectrons emitted by the photocathode. These photoelectrons are accelerated by a potential of the order of some tens of kilovolts and focused by electrostatic lenses on a visualisation screen, a small fluorescent screen (typical diameter one-inch), where the final image is obtained with a highly amplified luminance with respect to the initial one.

The final image, in the visualisation screen, can be of the order of several orders of magnitude more brilliant than in the fluorescent screen on the anterior face of the tube ($10 - 10^2 \text{ cd/m}^2$ for the former and 10^3 cd/m^2 for the latter). This image is directed to a TV camera through an optical coupling.

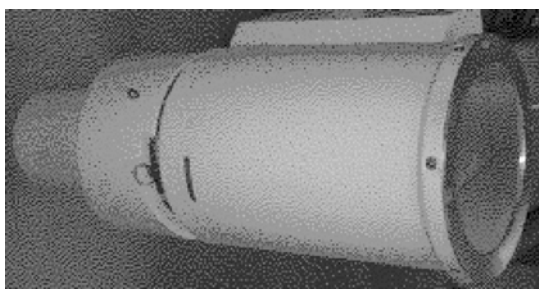


Fig. 7 - Photograph of a clinical image intensifier tube.

The overall setup of a digital fluorography system is schematised in Fig. 8. In this system the TV camera uses a vidicon (Fig. 9) and analogue to digital conversion of the video signal.

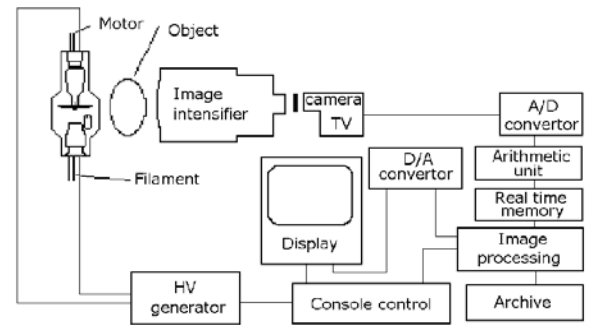


Fig. 8 - Block diagram of a digital fluorography system using a conventional TV camera.

The main components of a vidicon tube are shown in Fig. 9.

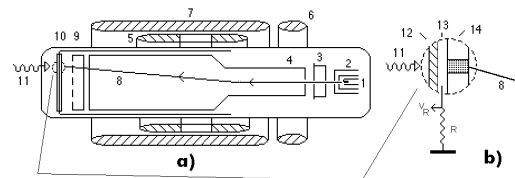


Fig. 9 - a) Schematic representation of a vidicon. 1-Filament; 2-First grid; 3-Second grid; 4- Cilindric electrode; 5- Deflection coil; 6- Correction coil; 7- Focusing coil; 8-Scanning electron beam; 9- Equalisation grid; 10- Detection electrode. b) Detail of a). 11-Light photons; 12-Glass; 13-Conductive and transparent layer of Al_2O_3 ; 14- Photoconductive electrode.

With the introduction of digital TV cameras with CCD's (charge coupled devices), the logic for pixel addressing is simplified. CCD's are integrated circuits consisting of electrodes (gates) on a semiconductor substrate forming an array of MOS capacitors, Fig. 10. Applying voltages to the gates, the material below is depleted to form charge storage 'wells'. Charge is generated within the semiconductor by the photoelectric absorption of light quanta. The charge can be changed from well to well, under the gates, applying voltage pulses between adjacent gates.

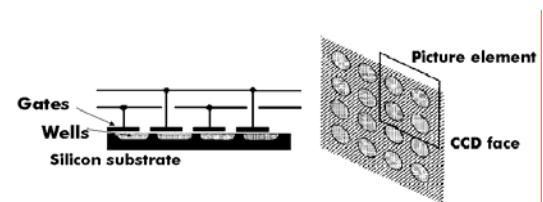


Fig. 10 - Schematic drawing of a CCD circuit.

Attempts have been made to develop systems based upon the optical coupling of charge coupled devices

(CCD) to scintillators. A disadvantage of these devices results from the extreme optical reduction factors caused by the relatively small CCD surface areas.

VII. IMAGE PLATE

In 1983 Fuji Laboratories developed an erasable X-ray imaging device based on the X-ray excitation of a phosphor layer and subsequent reading the stored image data with an infra-red laser (photo-stimulated luminescence). Results showed the imaging plate was more sensitive than conventional X-ray film with intensifying screens (Fig.11).

The image plate sensitivity is far superior to film/screen. Plots of exposure vs. response (dynamic range) show the increase in sensitivity and the extended response of the image plate for very low radiation doses. The practical dynamic range is 1:10000 compared to film/screen of 1:1000. The response of the luminescence is linear from 8 X-ray photons per pixel to 4×10^4 photons per pixel, a range of 1 to 2×10^3 .

The photostimulable luminescence (PSL) light whose intensity is proportional to the initial X-ray exposure is detected by a FM tube, generating an electric signal.

Position and PSL intensity are the information supplied by the image plate.

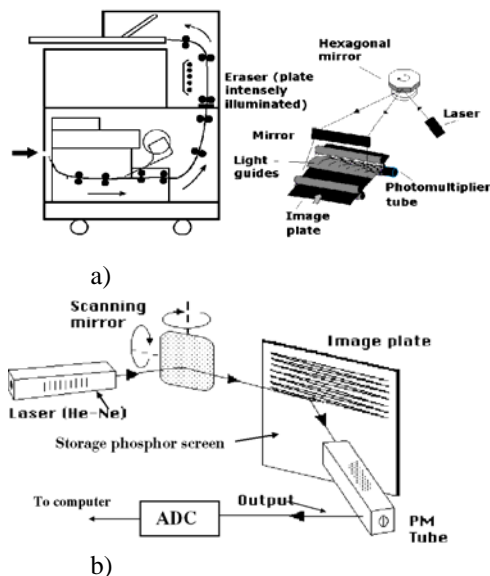
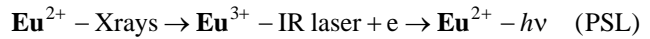


Fig. 11 - a) Diagram of the process in photo-stimulated luminescence based image plate. b) Detail of the reading step.

The phosphor material used for the image plate is a complex barium halide doped with europium. When the imaging plate absorbs X-ray energy some of the Eu^{2+} ions are oxidised to Eu^{3+} liberating electrons to the conduction band of the phosphor crystals. Some electrons are trapped at impurity levels in the forbidden zone, called F centres which are very long life energy states. Exposure to infrared light releases the trapped

electrons from the F-centres in the crystal, back to the conduction band where they convert the Eu^{3+} back into Eu^{2+} emitting characteristic radiation of europium at 390 nm as luminescent light. Excited molecules of BaFBr:Eu^{3+} , need stimulation radiation, with λ from 500 - 750 nm. Infrared He-Ne laser (633 nm) is a convenient energy source (Fig. 12). Reactions with Eu ions are indicated below



Scanning the plate with an infra-red laser beam (He-Ne) the trapped electrons are liberated to the conduction band and return to the valence band emitting UV photo-stimulated luminescence.

The physical phenomena behind photostimulable luminescence is thermoluminescence.

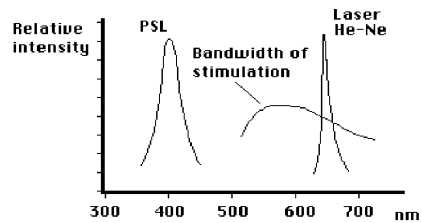


Fig. 12 - Bandwidth of stimulation, He-Ne laser spectrum and photo stimulable luminescence

The very essence of the method is that the 400 nm BaFBr:Eu^{2+} PSL (photo stimulable luminescence) has intensity proportional to the original X-ray exposure. This relationship is quite close, only small losses due excited electrons missing the traps and returning directly to the valence band contribute to a minor error.

Some construction details of an image plate are shown in Fig. 13. The image plate consists of three layers:

- A protective layer for physical agents (abrasion, chocks, etc.)
- A layer of phosphor crystals
- A conductive layer, which absorbs light and avoids electrostatic discharges.

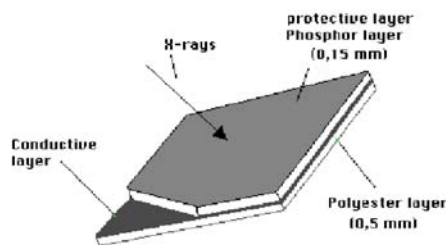


Fig. 13 - Construction details of an image plate.

The response time of the PSL is fast ($0.8 \mu\text{s}$) so it is possible to read many megabytes of image data within a few seconds using a scanning laser beam

Commercial image plates offer matrix sizes of 1760x2140 for standard resolution (ST) and 2000x2150 for high resolution (HR), at 10 bits. The effective resolution is 2.5 Lpmm⁻¹ for 35x43 cm ST plates and 5 Lpmm⁻¹ for 18x24 cm mammography HR plates.

Chest conventional X-ray systems commonly employ a 3584x4096 by 12 bit deep matrix having 5-10 pixel/mm resolution.

In the table below dimensions of existing image plates, and data on the matrices used are presented.

Dim. (cm)	Matrix	Pixel (mm)	Pixels/mm
35x43	1760x2140	0.2	5
35x35	1760x1760	0.2	5
24x30	1576x1976	0.15	6.7
18x24	1770x2370	0.1	10
18x24	1770x2370	0.1	10
20x25	2000x2510	0.21	10

Although distinguished by a high dynamic range and linearity this technology still requires handling since the initially stored analog image has to be converted into a digital matrix by a laser beam reader.

These storage phosphor systems, developed about 16 years ago, were the first step with practical applicability in filmless digital radiology but it is felt that the new advances recently announced can improve considerably these techniques.

VIII. IMAGE ACQUISITION MODALITIES AND DETECTION SYSTEMS IN DIGITAL RADIOLOGY

Several types of digital detectors have been developed for radiological purposes. Taking into account the physical detection steps and the acquisition modalities one can consider the following types

- One stage acquisition systems
- Two stage acquisition systems

and these can be

- Area detectors
- Scanned detectors
- Hybrid systems

In one stage acquisition, X-ray photons are absorbed by a matrix of detectors supplying directly an electric signal.

In two stage acquisition X-ray photons are absorbed by a scintillator (such as CsI) and the emitted light detected by photosensitive TFT (thin film transistor) arrays.

In area detectors, the information is acquired and processed simultaneously in every point of the detector area.

In scanning detectors information is read from the detection area by means of a scanning system.

Hybrid systems have some degree of superimposition of these characteristics.

A. Important image properties

A radiologic imaging device can be perfectly characterised, as far as sensitivity and spatial resolution are concerned, by its point response function B(x), that is the function describing the image when the object is an X-ray absorbing point source. Resolution distance **d** is the width at half-height of curve B(x). Two point-objects at distance **d** are barely separated in the image, Fig. 14.

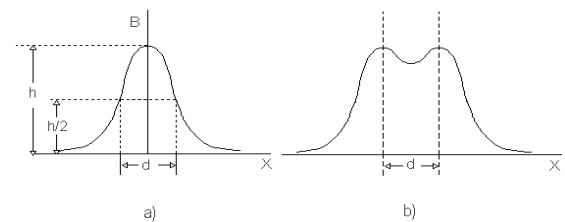


Fig. 14 - **a)** Resolution distance **d** is the full width at maximum half height of curve B(x). **b)** Two point objects at distance **d** are barely separated at the image.

A perfect radiologic imaging system would give a point image for every point source but, in practical devices, degradation occurs and the images of points appear as broad density distributions.

Every distribution of absorbing matter can be represented as a set of point objects and the blurring of images of extended sources in practical devices results from the mutual overlapping of the images of neighbouring point objects.

The total information contained in B(x) described above, is not easily used in a direct way.

It is also common practice to use another function, the modulation transfer function (MTF) which for some purposes has shown to be more convenient.

The MTF is based upon the principle that all distributions of absorbent material may be expressed as a summation of sinusoidal absorbent components each having a different spatial frequency. Distributions with sharp variations in atomic number, or thickness, or exhibiting fine detail have, generally, high frequencies in their spectral content, whereas coarse objects have mainly low frequency components.

It is assumed also that the images are more or less close descriptions of the objects in terms of superimposed sine wave components. On the other hand images of simple sinusoidal structure objects can be compared to evaluate the response. The MTF expresses the response of the system, or system components, to sinusoidally modulated distributions of thickness (Fig. 15) when the spatial frequency is varied.

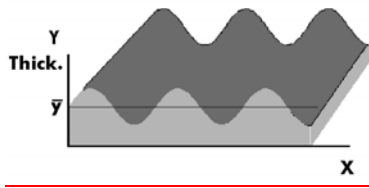


Fig. 15 - Absorber with sinusoidally modulated thickness in XX direction.

For every value of spatial frequency the MTF is the ratio of the modulations or contrasts of image and object (Fig. 15). Modulation of sinusoidal variation of density is defined as the ratio of the AC component of the density (one half of the peak to peak density) to the average density or DC component.

It was assumed above that the image of a sinusoidally modulated object is a sinusoidally modulated image of the same frequency although amplitude and phase can be different. Then

$$MTF = \frac{\text{Image modulation}}{\text{Object modulation}}$$

MTF is a decreasing function of frequency. For spatial frequencies above a certain value f_c , called the cut frequency, the object contrast is not transmitted to image, the MTF is null.

The cut frequencies for some imaging diagnostic methods are listed below:

- Film without intensifier screen: 100 lines/mm
- Film with intensifier screen: 8 -14 lines/mm
- Image intensifier de: 1 - 2 lines/mm
- CT scanner: 1-2 lines/mm
- Gamma camera: 0.2 lines/mm

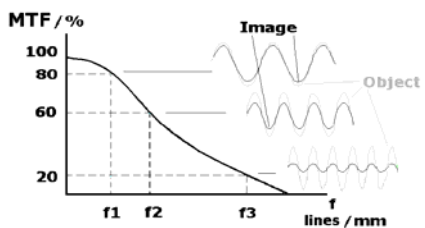


Fig. 16 - Modulation transfer function

B. Information transfer

Information transfer in an image intensifier tube system leads to heavy losses when compared with the new systems with digital detection. The successive transfer

steps in the image intensifier system result in about 63% losses.

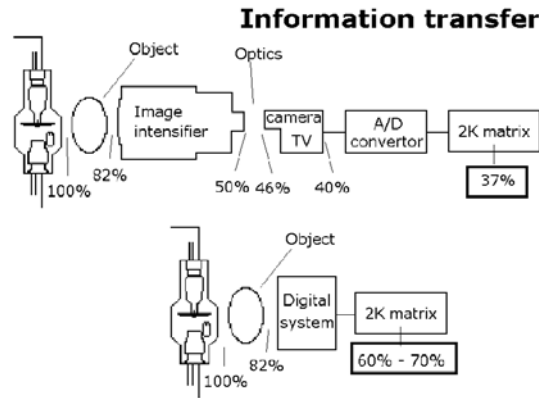


Fig. 17 - The successive transfer steps in the image intensifier system result in about 63% losses. With the new systems with digital detection losses are about 30%.

The point spread functions for the different solutions in diagnostic X-rays detectors are shown, in simplified terms, in Fig. 17.

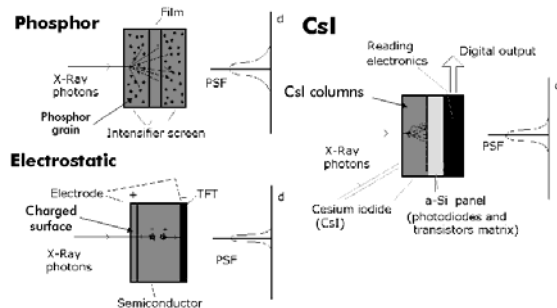


Fig. 18 - Point spread functions for the different solutions in diagnostic X-rays detectors.

It is seen that theoretically the most promising techniques in what concerns spatial resolution are those based on direct charge collection. The techniques that use luminescent detectors have inherent problems related with the light spread, a cause of spatial resolution deterioration, and also in the coupling of a light emitting electrode with the next stages, a cause of sensitivity loss (Fig. 19).

Medical images are two dimensional mappings of properties of the regions under study. These properties appear as functions of x and y, the position variables (fig. 20). The function values, in the pixels, represent a mean propriety in a voxel. The voxels depends on the technique used. In digital radiography a dimension is stolen to the object: the voxel is 3D and the pixel 2D.

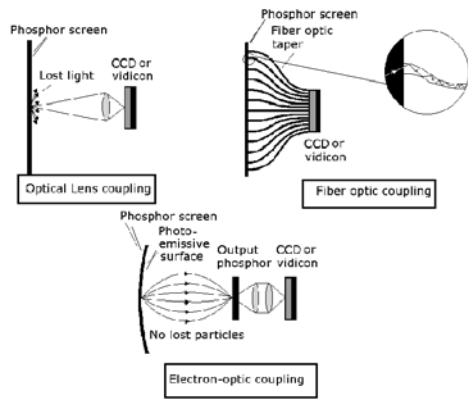


Fig. 19 - Types of light coupling used in medical X-ray detectors.

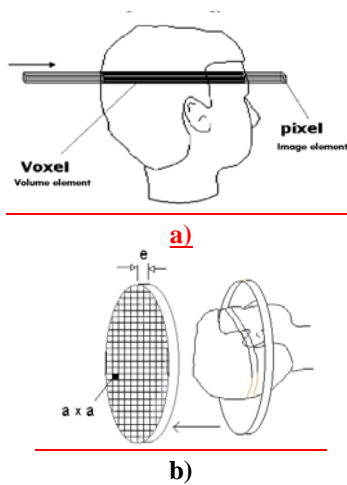


Fig. 20 - Pixel and voxel in: a) digital radiography; b) CAT.

C. Amorphous silicon solid-state detectors

The most promising technological approach up to now, in radiologic digital acquisition is the new two stage area detector, based on cesium iodide scintillators in combination with photosensors having an active amorphous silicon (a-Si) readout matrix (amorphous silicon solid-state detectors). The rapidly expanding market for active matrix liquid crystal displays has been a major driving force over the last decade for the a-Si thin film development.

The CsI absorbs X-ray photons and converts them to light. A needle like CsI structure inimises scattering. An array of low noise photodiodes receives this light and converts it into an electric signal. Each photodiode represents a pixel. The signal at each pixel is read out digitally by low noise electronics and sent to the image processor. This technology has the potential to cover the entire range of applications required for general diagnosis: high patial resolution, high frame rate and good SNR transmission.

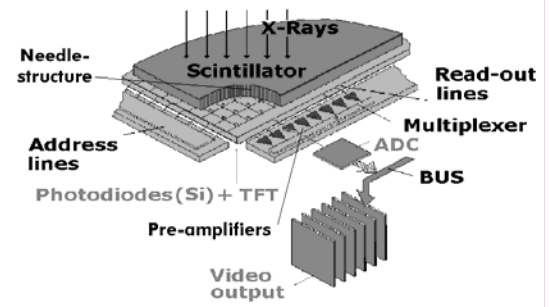


Fig. 21 - Schematic diagram of a CsI(a-Si) detector.

In fact, high DQE(f) and fast imaging rates make possible the use of amorphous silicon solid-state detectors in radiographic and fluoroscopic imaging.

Receiver operating characteristics analysis carried out on several X-ray diagnostic studies, have shown dose reduction without loss of diagnostic accuracy.

D. Selenium plate; amorphous-selenium (a-Se) area detector

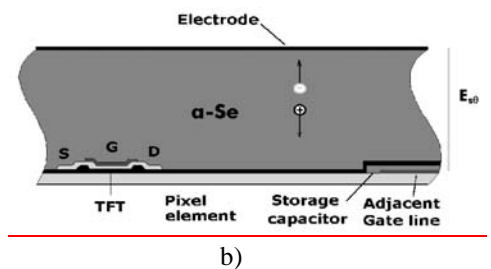
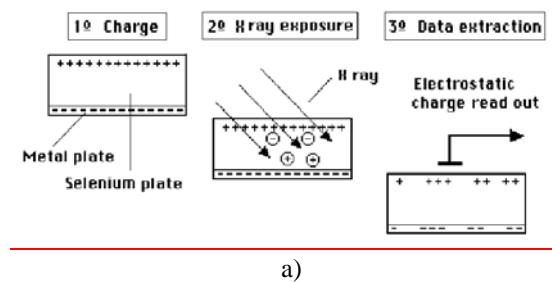


Fig. 22 - Scheme of the a-Se area detector.

Another approach is based on amorphous selenium, in which X-ray energy is directly converted into electric charge which is electrostatically sampled or read out by a matrix of active switching devices (active matrix).

The Se flat panel detectors consist of a photoelectric surface material (amorphous selenium) and a laminated array of thin film transistors (TFTs) with detector elements 0.15mmx0.15mm in size (Fig. 22 a and b).

In Fig. 22 a) the sequence of steps can be seen: 1) The surface is uniformly charged leading to about 1500 V between electrodes. 2) The charged plate is exposed to X-rays. ionising events produce local discharge of the plate. 3) The plate is scanned with a small electrode assembly in a pattern similar to the image plate laser or

directly read by a matrix of active switching devices. In the first case the surface is scanned in about 10 seconds.

The obtainable SNR at the current state of technology, makes questionable its fluoroscopic application. The electrical image is a matrix of typically 2000×2000 pixels. Each pixel representing about 0.2 mm and 14 bits deep.

The selenium image flat panel has a dynamic range equivalent to the image phosphor plate. However, selenium has low Z and therefore is a poor X-ray absorber and, consequently, the detector efficiency is low.

DQE is 0.25 at 2Lp mm⁻¹ for a dose of 3.3 mGy.

E. Comparing different detectors

In Table 2 are indicated typical matrix sizes in some radiological techniques. The values indicated for film and TV are the equivalent digital matrix sizes to have identical images.

Table 2

Rec. medium	Matrix size	Nr pixels	Pixels/m
Film 14"×17"	3500×4000	14 M	10
Image plate	2048×2048	4 M	4
625 lines TV	512×512	262 k	1
1249 line TV	1024×1024	1 M	2

The equivalent matrix for film is the largest one available, however, the information present is noisy and difficult to handle.

Dynamic range for image plate, film and image intensifier tube can be obtained from Fig. 23.

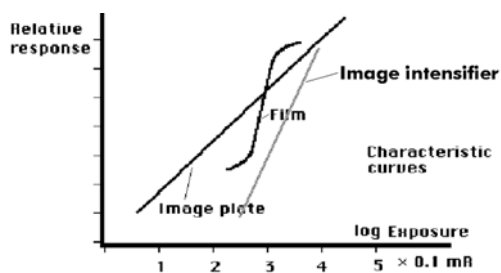


Fig. 23 - Dynamic range for image plate, film/screen and image intensifier tube.

Digital X-ray detectors can successfully image areas that might be under or over exposed on film and can further improve their display via image processing and window levelling. Digital X-ray detectors can successfully image areas that might be and can further improve their display via image processing and window levelling.

The detective quantum efficiency DQE(f) for film/screen and for the image plate, a-Se flat-panel and for the CsI (a-Si) digital detectors are shown in Fig. 24. It is evident that the last has the better response. The Se detector, or better, the semiconductor one stage electrostatic detectors, although having potentially spatial resolution advantages are not yet optimised enough to beat the CsI(a-Si) detectors. Screen/film detection and image plates have performances substantially poor when compared with the new generations.

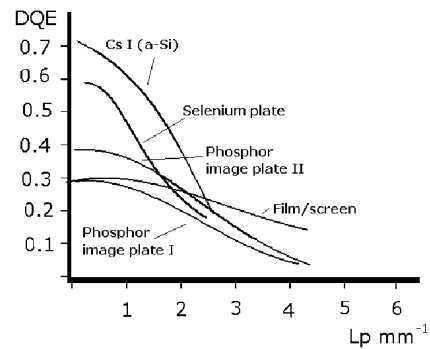


Fig. 24 - DQE(f) for some of the detectors studied, showing the superiority of Amorphous silicon solid-state detectors.

Everything indicates that the filmless radiography and the new digital techniques using new semiconductor or luminescent detectors and amorphous silicon technology are the future in X-ray imaging.

REFERENCES:

- [1] Dowsett DJ, Kenny PA and Johnston RE, "The Physics of Diagnostic Imaging", Chapman & Hall Medical. London, 1998 .
- [2] Yaffe MJ & Rowlands JA, "X-ray detectors for digital radiography", Phys. Med. Biol. **42** 1-39, 1997.
- [3] "Introduction to Digital X-ray imaging", GE Medical systems, 98-5488 11/98, 1998.
- [4] Spahn M, Alexander J, Gmeinwieser J, "Amorphous silicon solid-state detectors and their future application in Medical X-ray imaging", Electromedica **65**, 37-41, 1997.
- [5] Strotzer M, Gmeinwieser J, Spahn M, VolK M, Frund R, Seitz J, Spies V, Alexander J, Feuerbach S, "Amorphous silicon, flat-Panel, X- ray detector versus screen-film radiography", Invest. Radiol. **33**, 33-38, 1998
- [6] VolK M, Strotzer M, Gmeinwieser J, Alexander J, Frund R, Seitz J, Manke C, Spahn M, Feuerbach S, "Flat-panel X-ray detector using amorphous silicon technology", Invest. Radiol. **32**, 373-377, 1997.